J Nanopart Res (2015) 17:157
DOI 10.1007/s11051-015-2928-2

RESEARCH PAPER

Growth of silver-coated gold nanoshells with enhanced linear and nonlinear optical responses

Ya-Fang Zhang · Jia-Hong Wang · Liang Ma · Fan Nan · Zi-Qiang Cheng · Li Zhou · Qu-Quan Wang

Received: 29 September 2014 / Accepted: 21 February 2015 / Published online: 21 March 2015

Abstract Silver-coated gold nanoshells with 1,4-BDT molecules as the spacer (Ag/BDT/Au) were synthesized on the surface of SiO_2 nanospheres. The surface plasmon resonance of Au/SiO_2 and Ag/BDT/Au/SiO_2 nanoparticles with single and double shells were tuned by adjusting the thickness of Au and Ag nanoshells. The enhanced local field in the gap of Au and Ag shells is demonstrated by measuring Raman scattering and nonlinear refraction. The results show that the Raman intensity is enhanced by 17 times and the nonlinear refractive index is enhanced by 30 % due to the growth of Ag shells.

Keywords Gold nanoshells · Silver nanoshells · Surface plasmon resonance · Nonlinear refraction · Raman scattering

Y.-F. Zhang · J.-H. Wang · L. Ma · F. Nan · Z.-Q. Cheng · L. Zhou (✉) · Q.-Q. Wang (✉)
Department of Physics, Key Laboratory of Artificial Miro- and Nano-structures of the Ministry of Education, and School of Physics and Technology, Wuhan University, Wuhan 430072, People's Republic of China
e-mail: zhouli@whu.edu.cn

Q.-Q. Wang
e-mail: qqwang@whu.edu.cn

Introduction

Metallic nanoparticles have fascinated researchers for several decades because of their wide range of potential applications (Patolsky et al. 2004; Narayanan and El-Sayed 2005; Park et al. 2007; Aslan et al. 2007; Le et al. 2008; Ashayer et al. 2010; Nghiem et al. 2010; Pyne et al. 2011; Chu et al. 2011; Sun et al. 2014a, b). The properties of metallic nanoparticles are critically dependent on their composition, shape, geometry (Link and El-Sayed 2000; Jackson et al. 2003; Sosa et al. 2003; Cui et al. 2006; Karvianto and Chow 2012). In previous works, various morphologies have been developed, such as rods, cubes, triangles, cages, and so on (Busbee et al. 2003; Shankar et al. 2005; Chen et al. 2007; Li et al. 2010; Liu et al. 2013; Sun et al. 2014a, b). In particular, metal nanoshell is a subject with intensive experimental and theoretical studies in last two decade since the first report about Au/SiO_2 nanostructures by Oldenburg et al. (1998). The silica-metal nanoshells exhibit tunable surface plasmon resonances ranging from visible to infrared region by varying the composition, core size, and shell thickness. (Oldenburg et al. 1998; Pham et al. 2002; Lu et al. 2003; Phonthammachai et al. 2008; Liang et al. 2011; Gomez et al. 2012; Brito-Silva et al. 2013; Nghiem et al. 2013) Furthermore, the metal nanoshells have been widely used for plasmon-exciton coupling (Fofang et al. 2008, 2011), catalysis (Deng et al. 2007), chemical sensing (Raschke et al. 2004), biosensor (Shen et al. 2012), drug delivery (Bikram et al. 2007),

photothermal therapy (Coughlin et al. 2014), surface-enhanced Raman scattering (SERS) (Jackson and Halas 2004; Zhang and Guo 2009), and all-optical magnetic recording (Mayergoyz et al. 2009).

Surface plasmon resonance (SPR) of metal nanoshells strongly enhances the local electric field, which can be significantly improved by multishell coating. For instance, Da-Jian Wu et al. studied the plasmon coupling in a three-layered Au/SiO_2/Ag nanoshell by means of Mie scattering theory and found strong near-field enhancements in infrared region (Wu et al. 2011). Zhao's group studied the SPR properties of Au–Ag bimetallic multishell nanostructures theoretically and employed this nanostructure for SERS and surface-enhanced fluorescence (SEF) (Zhu et al. 2012). Sun's and Yao's groups prepared Fe_3O_4/Au/Ag multi-core/shell nanoparticles and used them for SERS and magnetic separation (Zeng and Sun 2008; Han et al. 2012). Furthermore, Shen et al. prepared Fe_3O_4@Ag/SiO_2/Au core–shell microspheres that display long-range plasmon transfer of Ag to Au, the novel multifunctional microspheres have proved to be efficient SERS-active substrate (Shen et al. 2013). The nonlinear optical responses of gold nanoshells also have been studied in recent years (Gordel et al. 2014); however, the nonlinearity optical properties enhanced by the plasmonic multishells have been seldom explored.

In this article, we described a facile method to prepare water-soluble silver-coated gold nanoshells. Tunable plasmon band arise from various silver thicknesses have been achieved. SERS activities and third-order nonlinear optical properties of Au nanoshells and Ag-coated Au nanoshells were obtained and compared for investigating the local field enhancement in the gap region between the Au shells and the Ag coating. It was found that the Raman intensity of 1,4-BDT was enhanced 17 times while the maximum effective nonlinear refractive (NLR) coefficient was enhanced by 30 %.

Experimental section

Materials

All chemicals were used as obtained without further purification. Potassium carbonate (K_2CO_3, 99.0 %), aqueous ammonia ($NH_3 \cdot H_2O$, 25–28 %), polyvinylpyrrolidone (PVP, average Mw–55,000), anhydrous toluene (99.8 %), silver nitrate ($AgNO_3$, 99.8 %), L-ascorbic acid (99.7 %), hexadecyltrimethylammonium (CTAC, 98.0 %), anhydrous ethanol, chloroauric acid ($HAuCl_4 \cdot 3H_2O$, 99.999 %), and 1,4-benzenedithiol (1,4-BDT, 98.0 %) were purchased from Sinopharm Chemical Reagent Co. Ltd. (Shanghai, China). Sodium borohydride ($NaBH_4$, 98.0 %) and tetraethyl orthosilicate (TEOS, 99.0 %) were obtained from Aldrich (America). 3-aminopropyltrimethoxysilane (APTES, 99 %) was purchased from Aladdin. (Shanghai, China). Ultrapure water with a resistivity of about 18.25 MΩ cm was used as the solvent in all experiments.

Preparation of Au/SiO_2 nanoshells

The Au/SiO_2 nanoshells were prepared according to the method described by Alexandre and co-workers (Brito-Silva et al. 2013) with some modifications. Specifically, silica nanospheres were prepared by mixing $NH_3 \cdot H_2O$ (28 %), anhydrous ethanol, and TEOS in a 50 mL plastic tube. The solution was sonicated for 2 h and the clear solution gradually turned opaque white due to the formation of silica suspension. The average diameter of silica spheres prepared by this method is about 110 nm. After centrifugation, the silica nanospheres solution was poured into a 100 mL round-bottom flask, and 2 mL of APTES was injected. The mixture was mingled under vigorous magnetic stirring at 110 °C for 12 h. Then, the amino-terminated silica nanoparticles (silica–NH_2 nanoparticles) were centrifuged at 6000 rpm for 13 min for three times. To prepare aqueous solution of gold colloids (2–3 nm in diameter), fresh prepared ice-cold $NaBH_4$ aqueous solution was poured into the mixture of PVP and $HAuCl_4$ rapidly, and stirring vigorously for 15 min. The resulting solution was stored in the refrigerator at 4 °C.

To link gold colloids on silica nanosphere, 30 mL of gold colloids was mixed with 5 mL of the as-prepared silica–NH_2 particles in a 100 mL glass beaker. The mixture was magnetic stirred for 2 h and centrifuged at 5500 rpm for 12 min. The precipitate was redispersed in 3 mL ultrapure water by sonication and mixed with 30 mL gold colloids under magnetic stirring for 2 h. The process was repeated four times to ensure the adsorption of AuNPs was completely accomplished. The precipitate was washed by water to remove the unabsorbed gold colloids and

redispersed in 2 mL of ultrapure water. The resulting solution (denoted by silica-Au precursor) was stored in a dark brown glass tube at 4 °C.

To prepare the growth solution, 50 mg of K_2CO_3 was dissolved in 200 mL of ultrapure water in a 250 mL beaker. After shaking gently, 3 mL of 20 mM $HAuCl_4$ was added and gently swirled. The resulting solution was stored in dark at room temperature and used within 2–5 days.

To grow Au nanoshells, different volumes of silica–Au precursor were injected into 5 mL of the growth solution. After the solution was mixed by agitation, 150 μL of 10 mM freshly prepared ice-cold $NaBH_4$ was added dropwise. The solution changed from colorless to green within 10 min, indicating the formation of Au nanoshells. After 2 h incubation, the products (named by Au/SiO_2 nanoshells) were centrifuged at 3800 rpm for 8 min and redispersed in ultrapure water for further use.

Preparation of silver-coated gold nanoshells (Ag/BDT/Au/SiO_2 nanoshells)

5 mL of the as-prepared gold nanoshell aqueous solution was mixed with 5 mL of 20 μM 1,4-BDT ethanol solution. The incubation time was kept for 1 hour in order to facilitate conjugation of 1,4-BDT onto the surface of gold nanoparticles. The resulting solution was centrifuged at 3800 rpm for 8 min and redispersed in 5 mL of ultrapure water (denoted by BDT/Au/SiO_2 nanoshells). The silver-coated gold nanoshells (Ag/BDT/Au/SiO_2 nanoshells) were prepared via reduction of $AgNO_3$ on gold by ascorbic acid. First of all, solution A and solution B were prepared. Solution A is formed by mixing 0.1 M ascorbic acid and 0.2 M CTAC together (the volume ratio is 3:2). Solution B is the aqueous solution of 0.01 M $AgNO_3$. 2 mL of solution A and certain volume of solution B were injected drop by drop into the 5 mL of Au nanoshells solution simultaneously. The mixture was stirred for 3 h at room temperature. The resulting solution was centrifuged at 3400 rpm for 7 min and redispersed in 5 mL of ultrapure water.

Characterization

Transmission electron microscopy (TEM) images were taken on a JEOL 2010 HT transmission electron microscope at an accelerating voltage of 200 kV. Absorption spectra were taken on a TU-1810 UV–Vis–NIR spectrophotometer (Purkinje General Instrument Co. Ltd. Beijing, China). Dynamic light scattering (DLS) measurements were performed with a Zeta sizer (Nano ZS90, Malvern Instruments, UK) at 25 °C. Raman spectra were obtained using a Confocal Raman Microspectroscopy (RM-1000), the excitation wavelength was 514.5 nm from an Ar^+ laser. Nonlinear optical properties of the obtained nanoshells were characterized using a home-made femtosecond Z-scan experiment. The excitation laser of 100 fs pulse with 76 MHz repetition rate was generated by a mode-locked Ti: sapphire laser (Coherent, Mira 900).

Results and discussion

Nanostructures and plasmon resonances of Ag/BDT/Au/SiO_2 nanoshells compositions

As schematically shown in Fig. 1, the preparation of the *Ag/BDT/Au/SiO_2* nanoshells can be divided into four steps: (i) the synthesis of silica–Au precursor by the modification of Au colloids outside the silica–NH_2 nanoparticles; (ii) the formation of gold shell onto SiO_2 core by the epitaxial growth of Au shells; (iii) the conjugation of 1,4-BDT onto Au/SiO_2 nanoshells; and (iv) the coating of silver shell with different thicknesses onto BDT/Au/SiO_2 nanoshells.

The formation of Au nanoshells onto SiO_2 core was firstly introduced by Halas group (Oldenburg et al. 1998). The synthesis, properties, and applications of Au nanoshells have been studied for decades. The SiO_2 cores were firstly modified by the small Au colloids (silica–Au). Then, the epitaxial growth of Au shells was performed by injecting the silica–Au precursors into the growth solution. For tuning the thickness and plasmon resonance band of the Au/SiO_2 nanoshells, different volumes of silica-Au precursors (2.5–30 μL) was injected into 5 ml growth solution (Fig. 2). TEM images of three different growth stages illustrate the progression in metal nanoshells growth. The low-magnification TEM images demonstrate that the samples are well dispersed. The SiO_2 and Au could be distinguished easily because the contrast is obvious. The gold colloids covered the silica cores partially when the precursor is 15 μL (Fig. 2b, e) and the average thickness of gold shell layer is about 12 nm. As the volume of silica–Au precursor decreases to

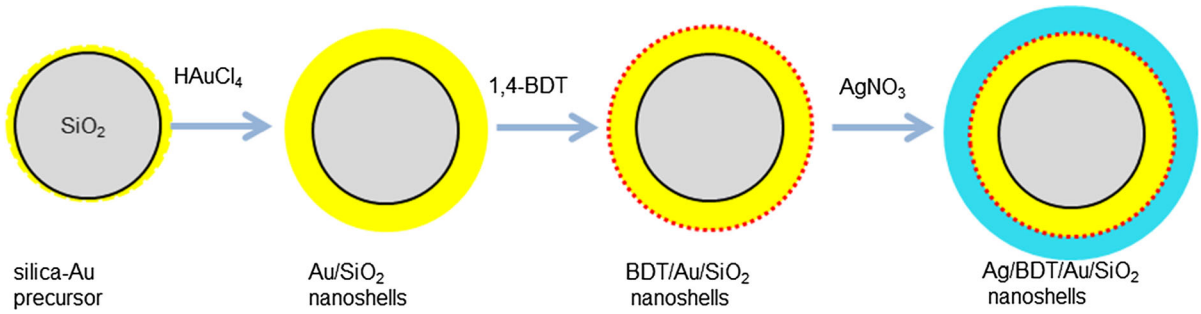

Fig. 1 A schematic illustration of the fabrication process of the samples

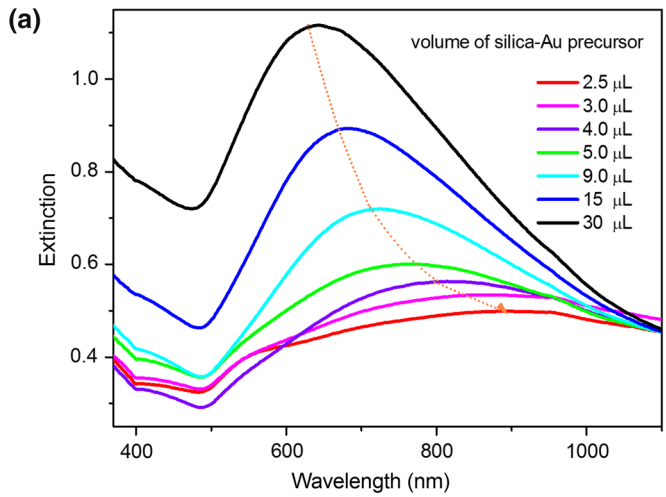

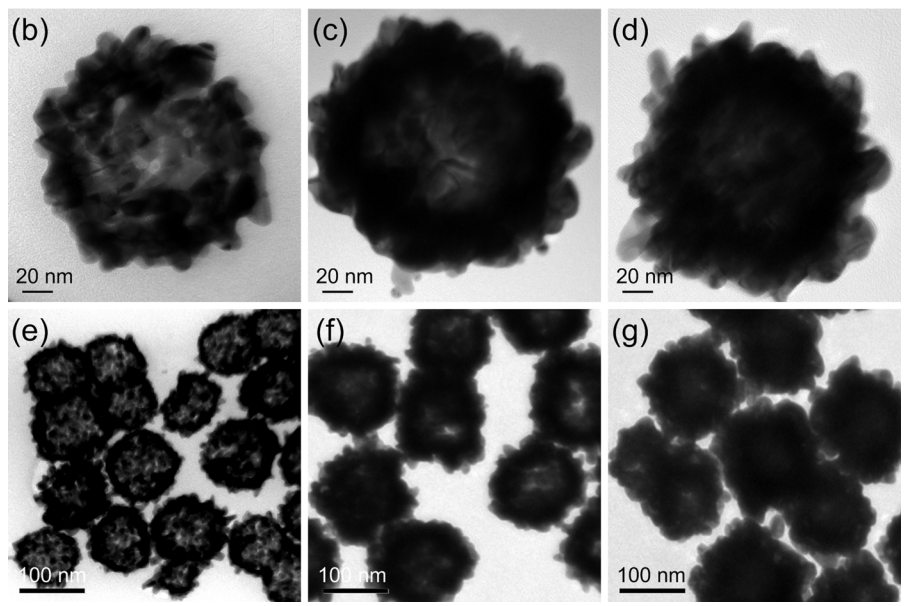

Fig. 2 **a** Extinction spectra of Au nanoshells growth on silica nanospheres with various precursor volumes. **b**–**g** Corresponding TEM images of the Au/SiO_2 nanoshells. The volumes of silica–Au precursor are **b**, **e** 15 μL, **c**, **f** 4 μL, and **d**, **g** 2.5 μL

4 μL, the gold network becomes more densely interconnected (Fig. 2c, f) and the average thickness of gold shell layer is about 29.5 nm. The nanoshells are nearly completed and the SiO_2 is hard to see except few of small pores when the silica-Au precursor is 2.5 μL and a uniform gold shell with thickness of 42 nm is formed (Fig. 2d, g). The controllable thickness of gold nanoshells results in tunable surface plasmon extinction bands in a wide range of wavelengths. As the gold nanoparticles coverage on the surface of SiO_2 increases, the plasmon resonance extinction spectra broaden and the main peak red shifts. Once the grown gold reaching a complete shell, the extinction spectra red shifts to a longer wavelength (902 nm). The similar phenomenon was observed and was explained by Averitt and the coworkers (Averitt et al. 1997).

Due to the existence of –SH group, 1,4-BDT molecules could be easily bonded onto the Au/SiO_2 nanoshells. The extinction spectra of Au/SiO_2 nanoshells show slight red-shift after the conjugation with 1,4-BDT (the absorption of 1,4-BDT is in the range of 250–350 nm). The as-prepared $BDT/Au/SiO_2$ nanoshells are used as seeds for the further growth of Ag shell. Due to the similar lattice constant between Au and Ag, the nucleation of Ag could be easily occured on the Au surface to form the external metallic shell. The thickness of Ag shell could be controlled by the amount of $AgNO_3$ in the reaction mixture. Various $Ag/BDT/Au/SiO_2$ nanoshell samples were synthesized and their extinction spectra were recorded, as presented in Fig. 3. Three representative TEM images from these samples are also shown in Fig. 3. Figure 3b and e is the TEM images of the initial $BDT/Au/SiO_2$ nanoshells, and they present maximum extinction in the long wavelength side (832 nm). Some pores that are not covered by Au nanoparticles are apparent in the TEM images. After the coating of Ag, the plasmon band exhibits blue-shift with enhanced extinction intensity, and an extinction shoulder is appeared at around 400 nm corresponding to Ag. The dielectric function of silver is different from gold; therefore, the variation of effective dielectric function accounts for the blue-shift phenomenon (Liu and Guyot-Sionnest 2004). After the coating of silver, the Au shells are hard to distinguish but the surface morphology of nanoshells becomes smoother. As shown in the TEM images, the pores in the starting $BDT/Au/SiO_2$ nanoshells gradually disappear and the overall diameter of nanoparticles become larger (the average diameter increase from 192.27 to 311.39 nm) and irregular. The Ag coverage increased from Fig. 3c, reaching the larger and more irregular nanoshells in Fig. 3d and g. Meanwhile, their SP extinction peak blue shifts to 600 nm and the band at 400 nm red shifts a little to 410 nm with the intensity being much stronger.

Meanwhile, DLS measurement was performed in order to determine the main particle size and the polydisperse property of the samples (see Fig. 4). From the results of DLS measurement, we can see that the average hydrodynamic diameter and polydisperse index (PDI) of Au/SiO_2 nanoshells sample shown in Fig. 2g are about 210 nm and 0.095 and that of the $Ag/BDT/Au/SiO_2$ nanoshells sample shown in Fig. 3f are about 300 nm and 0.241, which indicates that the samples have a good dispersion and the results are coincident with that measured by TEM.

Linear optical response with enhanced Raman signals

It is reported by Xu that the electric field could be enhanced in the gap region between a Ag core and a Ag shell (Xu 2005). In the present work, we use 1,4-BDT molecules located in the gap regions as Raman analytes to demonstrate the intense local field confined in the gaps between the Au and Ag layers. Figure 5 shows the Raman signals of 1,4-BDT modified Au/SiO_2 nanoshells before and after the Ag deposition. Since the two types of nanoshells are derived from the same $BDT/Au/SiO_2$ nanoshells sample, the coverage and density of 1,4-BDT are the same. It should be noted that all the samples labeled with 1,4-BDT are must be cleaned by centrifugation at least two times to discard the unbound molecule. The SP absorption bands of these two samples are 832 nm ($BDT/Au/SiO_2$ nanoshell) and 600 nm ($Ag/BDT/Au/SiO_2$ nanoshell). The Raman patterns corresponding to 1,4-BDT in Fig. 5 agree well with the previous report (Joo et al. 2001). The strongest peak at 1567 cm^{-1} attributed to the benzene ring mode was chosen for the calculation of enhancement factor of SERS. The Raman intensity of the $Ag/BDT/Au/SiO_2$ nanoshells is almost 17 times against than that from the $BDT/Au/SiO_2$ nanoshells. The large enhancement indicates that the region between Au and Ag layer may behave as a cavity to concentrate electromagnetic field. The results suggest that the $Ag/BDT/Au/SiO_2$ nanoshells are more

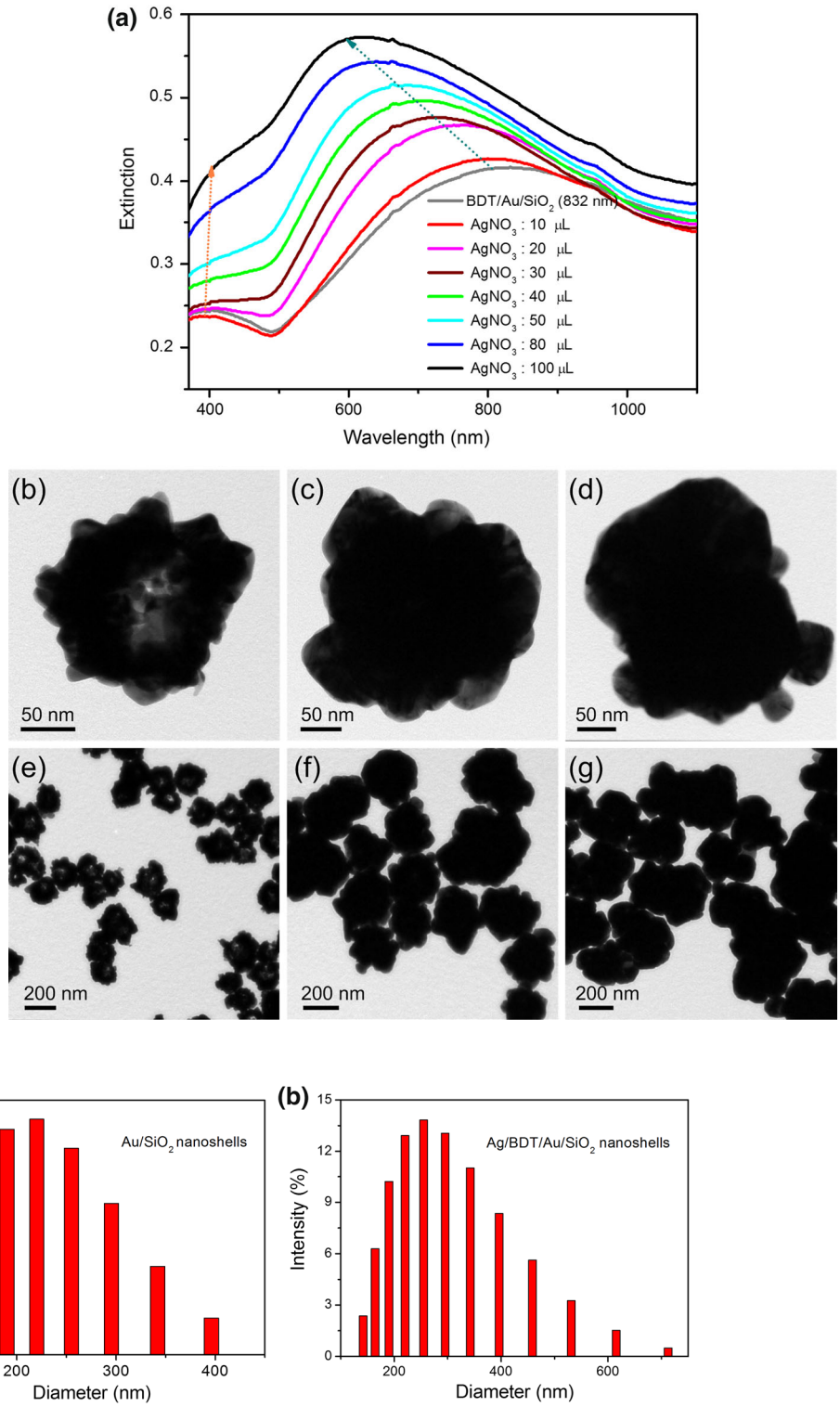

Fig. 3 **a** Extinction spectra of Ag/BDT/Au/SiO_2 nanoshells synthesized by different volumes of $AgNO_3$. **b**–**g** Corresponding TEM images of Ag/BDT/Au/SiO_2 nanoshells prepared by the addition of $AgNO_3$ with different volumes: **b**, **e** 0 μL; **c**, **f** 250 μL; **d**, **g** 500 μL

Fig. 4 **a** The size distribution of (**a**) Au/SiO_2 nanoshells sample shown in Fig. 2g and **b** Ag/BDT/Au/SiO_2 nanoshells sample shown in Fig. 3f determined by DLS

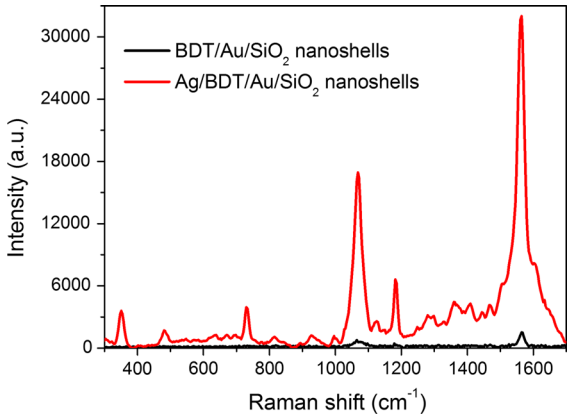

Fig. 5 SERS spectra of 1.0×10^{-5} mol L^{-1} 1,4-BDT adsorbed on Au/SiO_2 nanoshells nanoparticles before (*black*) and after (*red*) the addition of $AgNO_3$. (Color figure online)

suitable than $BDT/Au/SiO_2$ for using as SERS probe. In addition, it is known that the size of the nanoparticles is an important parameter of the field enhancement which has been studied in detail (Sant'Ana et al. 2009; Amendola and Meneghetti 2012; Shaw et al. 2013). Because the average size of $Ag/BDT/Au/SiO_2$ nanoshells is larger than that of $BDT/Au/SiO_2$ nanoshells, the size enlargement will also lead to the SERS enhancement. Furthermore, the excitation wavelength also is a possible factor for the enhanced SERS signal, because the plasmon band of $Ag/BDT/Au/SiO_2$ nanoshells is closer to 514.5 nm than that of Au/SiO_2 nanoshells.

Nonlinear optical response with enhanced nonlinear refraction

The field enhancement in these two samples used in Raman measurement can also be characterized using femtosecond Z-scan experiment. A mode-locked Ti:sapphire laser tuned to the resonance wavelength of the samples and delivering pulses of about 150 fs at a repetition rate of 76 MHz was focused into a 1-mm-thick quartz cuvette containing the sample solution. The photodegradation of the metal nanostructure under laser irradiation is a frequent problem and is more frequent for large particles. When the fluence of pulsed laser is larger than 200 mJ/cm^2, the laser-induced fragmentation of colloidal nanoparticles appears (Fujiwara et al. 1999; Mafuné et al. 2002; Besner et al. 2006; Amendola et al. 2009). To avoid the photodegradation of nanoshells, the laser power density was used as low as 0.63 GW/cm^2 for the Z-scan measurements. Power-dependent refractive index n of materials could be described as $n(I) = n_0 + \gamma I$, where n_0 represents the linear refractive index, γ is the nonlinear refraction coefficient, and I is the excitation laser power. Figure 6 presents the normalized T_{CL}/T_{OP} Z-scan curves related to γ of $BDT/Au/SiO_2$ nanoshells and $Ag/BDT/Au/SiO_2$ nanoshells samples with different excitation wavelengths. NLR index γ can be calculated by open-aperture transmittance T_{OP} and close-aperture transmittance T_{CL} as following relationships though the Z-scan theory:

$$\frac{T_{CL}}{T_{OP}} = 1 + \frac{4\Delta\phi_0 z/z_0}{\left[\left(z/z_0\right)^2 + 9\right]\left[\left(z/z_0\right)^2 + 1\right]},$$

where $\Delta\phi_0 = \gamma k I_0 L_{eff}$. I_0 is the peak irradiance at the focus ($z = 0$). L_{eff} is the effective thickness of the samples, $k = 2\pi/\lambda$ is the wave vector of the laser radiation, z_0 is the Rayleigh length of the Gaussian incident beam.

Self-defocusing effect curves of both $BDT/Au/SiO_2$ nanoshells and $Ag/BDT/Au/SiO_2$ nanoshells represent the negative values of NLR index. The values of γ in $BDT/Au/SiO_2$ nanoshells and $Ag/BDT/Au/SiO_2$ nanoshells samples are calculated to be about -0.7×10^{-4} and -0.91×10^{-4} cm^2/GW, indicating that the local field was enhanced due to the interaction between Au and Ag coating. In order to exclude the effect of the 1,4-BDT, we measured the Z-scan signals of 1,4-BDT with different concentrations and no

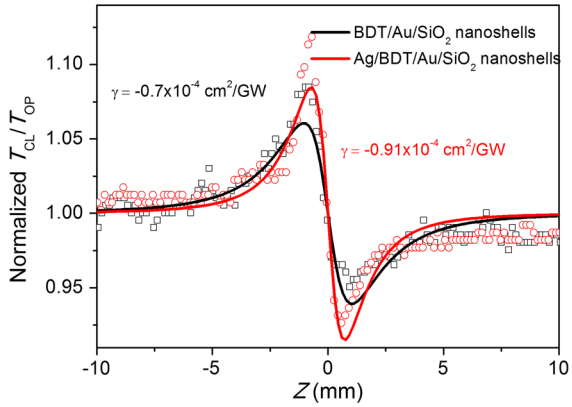

Fig. 6 Normalized T_{CL}/T_{OP} curves of $BDT/Au/SiO_2$ nanoshells nanoparticles before (*black*) and after (*red*) the addition of $AgNO_3$. The *scattered dots* are experimentally data while the *solid lines* are theoretically fitting curves. (Color figure online)

obvious nonlinear signals were observed; moreover, the NLR index of nanoshells with or without 1,4-BDT is similar. This demonstrates that the NLR index increase as high as 30 % is mainly contributed to the enhancement of electromagnetic field. However, the field enhancement is much lower than that calculated by SERS, the reason may be that the large scattering of Ag/BDT/Au/SiO_2 nanoshells decreased the effective irradiance energy and the equalization induced by the water solution.

Conclusion

In summary, we investigated enhanced linear and nonlinear optical responses of silver-coated gold nanoshells. The Au nanoshells were firstly grown on SiO_2 spheres by injecting the silica-Au precursors into the K_3CO_3–$HAuCl_4$ growth solution. The SPR could be tuned form 646 to 902 nm by adjusting the volume of silica-Au precursors. After the modification of 1,4-BDT molecules onto the surface of Au/SiO_2 nanoshells, Ag layer was deposited by reducing $AgNO_3$ with AA. The SPR of silver-coated gold nanoshells could be tuned from 832 to 600 nm by adjusting the amount of $AgNO_3$. Compared with the BDT/Au/SiO_2 nanoshells, the Raman intensity is enhanced by 17 times and the nonlinear refractive index is enhanced by 30 % for the Ag/BDT/Au/SiO_2 nanoshells.

Acknowledgments The authors thank Z H Hao, X L Liu, and S J Ding for their helpful assistance and discussions. This work was supported by the National Program on Key Science Research of China (2011CB922201), and the NSFC (61008043, 11174229, and 11204221).

References

Amendola V, Meneghetti M (2012) Exploring how to increase the brightness of surface-enhanced Raman spectroscopy nanolabels: the effect of the Raman-active molecules and of the label size. Adv Funct Mater 22:353–360. doi:10.1002/adfm.201101539

Amendola V, Dini D, Polizzi S, Shen J, Kadish KM, Calvete MJF, Hanack M, Meneghetti M (2009) Self-healing of gold nanoparticles in the presence of Zinc phthalocyanines and their very efficient nonlinear absorption performances. J Phys Chem C 113:8688–8695. doi:10.1021/jp810921w

Ashayer R, Green M, Mannan SH (2010) Synthesis of palladium nanoshell using a layer-by-layer technique. J Nanopart Res 12:1489–1494. doi:10.1007/s11051-009-9721-z

Aslan K, Wu M, Lakowicz JR, Geddes CD (2007) Fluorescent core-shell Ag@SiO2 nanocomposites for metal-enhanced fluorescence and single nanoparticle sensing platforms. J Am Chem Soc 129:1524–1525. doi:10.1021/ja0680820

Averitt RD, Sarkar D, Halas NJ (1997) Plasmon resonance shifts of Au-coated Au_2S nanoshells: insight into multicomponent nanoparticle growth. Phys Rev Lett 78:4217–4220. doi:10.1103/PhysRevLett.78.4217

Besner S, Kabashin AV, Meunier M (2006) Fragmentation of colloidal nanoparticles by femtosecond laser-induced supercontinuum generation. Appl Phys Lett 89:233122. doi:10.1063/1.2402944

Bikram M, Gobin AM, Whitmire RE, West JL (2007) Temperature-sensitive hydrogels with SiO_2–Au nanoshells for controlled drug delivery. J Control Release 123:219–227. doi:10.1016/j.jconrel.2007.08.013

Brito-Silva AM, Sobral-Filho RG, Barbosa-Silva R, de Araújo CB, Galembeck A, Brolo AG (2013) Improved synthesis of gold and silver nanoshells. Langmuir 29:4366–4372. doi:10.1021/la3050626

Busbee BD, Obare SO, Murphy CJ (2003) An improved synthesis of high-aspect-ratio gold nanorods. Adv Mater 15:414–416. doi:10.1002/adma.200390095

Chen JY, Wang DL, Xi JF, Au L, Siekkinen A, Warsen A, Li ZY, Zhang H, Xia YN, Li XD (2007) Immuno gold nanocages with tailored optical properties for targeted photothermal destruction of cancer cells. Nano Lett 7:1318–1322. doi:10.1021/nl070345g

Chu VH, Fort E, Nghiem THL, Tran HN (2011) Photoluminescence enhancement of dye-doped nanoparticles by surface plasmon resonance effects of gold colloidal nanoparticles. Adv Nat Sci 2:045010. doi:10.1088/2043-6262/2/4/045010

Coughlin AJ, Ananta JS, Deng NF, Larina IV, Decuzzi P, West JL (2014) Gadolinium-conjugated gold nanoshells for multimodal diagnostic imaging and photothermal cancer therapy. Small 10:556–565. doi:10.1002/smll.201302217

Cui Y, Ren B, Yao JL, Gu RA, Tian ZQ (2006) Synthesis of $Ag_{core}Au_{shell}$ bimetallic nanoparticles for immunoassay based on surface-enhanced Raman spectroscopy. J Phys Chem B 110:4002–4006. doi:10.1021/jp056203x

Deng ZW, Chen M, Wu LM (2007) Novel method to fabricate SiO_2/Ag composite spheres and their catalytic, surface-enhanced Raman scattering properties. J Phys Chem C 111:11692–11698. doi:10.1021/jp073632h

Fofang NT, Park TH, Neumann O, Mirin NA, Nordlander P, Halas NJ (2008) Plexcitonic nanoparticles: plasmon–exciton coupling in nanoshell–J-Aggregate complexes. Nano Lett 8:3481–3487. doi:10.1021/nl8024278

Fofang NT, Grady NK, Fan ZY, Govorov AO, Halas NJ (2011) Plexciton dynamics: exciton-plasmon coupling in a J-Aggregate–Au nanoshell complex provides a mechanism for nonlinearity. Nano Lett 11:1556–1560. doi:10.1021/nl104352j

Fujiwara H, Yanagida S, Kamat PV (1999) Visible laser induced fusion and fragmentation of thionicotinamide-capped gold nanoparticles. J Phys Chem B 103:2589–2591. doi:10.1021/jp984429c

Gomez L, Arruebo M, Sebastian V, Gutierrez L, Santamaria J (2012) Facile synthesis of SiO_2–Au nanoshells in a three-

stage microfluidic system. J Mater Chem 22:21420–21425. doi:10.1039/C2JM34206E

Gordel M, Olesiak-Banska J, Kolkowski R, Matczyszyn K, Buckle M, Samoc M (2014) Shell-thickness-dependent nonlinear optical properties of colloidal gold nanoshells. J Mater Chem C 2:7239–7246. doi:10.1039/C4TC01210K

Han SY, Guo QH, Xu MM, Yuan YX, Shen LM, Yao JL, Liu W, Gu RA (2012) Tunable fabrication on iron oxide/Au/Ag nanostructures for surface enhanced Raman spectroscopy and magnetic enrichment. J Colloid Interface Sci 378:51–57. doi:10.1016/j.jcis.2012.04.047

Jackson JB, Halas NJ (2004) Surface-enhanced Raman scattering on tunable plasmonic nanoparticle substrates. Proc Natl Acad Sci USA 101:17930–17935. doi:10.1073/pnas.0408319102

Jackson JB, Westcott SL, Hirsch LR, West JL, Halas NJ (2003) Controlling the surface enhanced Raman effect via the nanoshell geometry. Appl Phys Lett 82:257–259. doi:10.1063/1.1534916

Joo SW, Han SW, Kim K (2001) Adsorption of 1,4-benzenedithiol on gold and silver surfaces: surface-enhanced Raman scattering study. J Colloid Interface Sci 240:391–399. doi:10.1006/jcis.2001.7692

Karvianto, Chow GM (2012) Size-dependent transformation from Ag templates to Au–Ag nanoshells via galvanic replacement reaction in organic medium. J Nanopart Res 14:1186. doi:10.1007/s11051-012-1186-9

Le F, Brandl DW, Urzhumov YA, Wang H, Kundu J, Halas NJ, Aizpurua J, Nordlander P (2008) Metallic nanoparticle arrays: a common substrate for both surface-enhanced Raman scattering and surface-enhanced infrared absorption. ACS Nano 2:707–718. doi:10.1021/nn800047e

Li WB, Guo YY, Zhang P (2010) General strategy to prepare TiO_2-core gold-shell nanoparticles as SERS-tags. J Phys Chem C 114:7263–7268. doi:10.1021/jp908160m

Liang ZS, Liu Y, Ng SS, Li XY, Lai LH, Luo SF, Liu SY (2011) The effect of pH value on the formation of gold nanoshells. J Nanopart Res 13:3301–3311. doi:10.1007/s11051-011-0244-z

Link S, El-Sayed MA (2000) Shape and size dependence of radiative, non-radiative and photothermal properties of gold nanocrystals. Int Rev Phys Chem 19:409–453. doi:10.1080/01442350050034180

Liu MZ, Guyot-Sionnest P (2004) Synthesis and optical characterization of Au/Ag core/shell nanorods. J Phys Chem B 108:5882–5888. doi:10.1021/jp037644o

Liu XL, Liang S, Nan F, Yang ZJ, Yu XF, Zhou L, Hao ZH, Wang QQ (2013) Solution-dispersible Au nanocube dimers with greatly enhanced two-photon luminescence and SERS. Nanoscale 5:5368–5374. doi:10.1039/C3NR01170D

Lu LH, Sun GY, Xi SQ, Wang HS, Zhang HJ, Wang TD, Zhou XH (2003) A colloidal templating method to hollow bimetallic nanostructures. Langmuir 19:3074–3077. doi:10.1021/la026521c

Mafuné F, Kohno J, Takeda Y, Kondow T (2002) Growth of gold clusters into nanoparticles in a solution following laser-induced fragmentation. J Phys Chem B 106:8555–8561. doi:10.1021/jp020786i

Mayergoyz I, McAvoy P, Lang G, Bowen D, Krafft C (2009) Excitation and dephasing of circularly polarized plasmon modes in spherical nanoshells for application in all-optical magnetic recording. J Appl Phys 105:07B904. doi:10.1063/1.3068544

Narayanan R, El-Sayed MA (2005) Effect of colloidal nanocatalysis on the metallic nanoparticle shape: the Suzuki reaction. Langmuir 21:2027–2033. doi:10.1021/la047600m

Nghiem THL, La TH, Vu XH, Chu VH, Nguyen TH, Le QH, Fort E, Do QH, Tran HN (2010) Synthesis, capping and binding of colloidal gold nanoparticles to proteins. Adv Nat Sci 1:025009. doi:10.1088/2043-6254/1/2/025009

Nghiem THL, Le TN, Do TH, Vu TTD, Do QH, Tran HN (2013) Preparation and characterization of silica–gold core–shell nanoparticles. J Nanopart Res 15:2091. doi:10.1007/s11051-013-2091-6

Oldenburg SJ, Averitt RD, Westcott SL, Halas NJ (1998) Nanoengineering of optical resonances. Chem Phys Lett 288:243–247. doi:10.1016/S0009-2614(98)00277-2

Park HY, Schadt MJ, Wang LY, I-ImS Lim, Njoki PN, Kim SH, Jang MY, Luo J, Zhong CJ (2007) Fabrication of magnetic core@shell Fe oxide@Au nanoparticles for interfacial bioactivity and bio-separation. Langmuir 23:9050–9056. doi:10.1021/la701305f

Patolsky F, Weizmann Y, Willner I (2004) Actin-based metallic nanowires as bio-nanotransporters. Nat Mater 3:692–695. doi:10.1038/nmat1205

Pham T, Jackson JB, Halas NJ, Lee TR (2002) Preparation and characterization of gold nanoshells coated with self-assembled monolayers. Langmuir 18:4915–4920. doi:10.1021/la015561y

Phonthammachai N, Kah JCY, Jun G, Sheppard CJR, Olivo MC, Mhaisalkar SG, White TJ (2008) Synthesis of contiguous silica-gold core-shell structures: critical parameters and processes. Langmuir 24:5109–5112. doi:10.1021/la703580r

Pyne S, Sarkar P, Basu S, Sahoo GP, Bhui DK, Bar H, Misra A (2011) Synthesis and photo physical properties of Au@Ag (core@shell) nanoparticles disperse in poly vinyl alcohol matrix. J Nanopart Res 13:1759–1767. doi:10.1007/s11051-010-9955-9

Raschke G, Brogl S, Susha AS, Rogach AL, Klar TA, Feldmann J, Fieres B, Petkov N, Bein T, Nichtl A, Kürzinger K (2004) Gold nanoshells improve single nanoparticle molecular sensors. Nano Lett 4:1853–1857. doi:10.1021/nl049038q

Sant'Ana AC, Rocha TCR, Santos PS, Zanchet D, Temperini MLA (2009) Size-dependent SERS enhancement of colloidal silver nanoplates: the case of 2-amino-5-nitropyridine. J Raman Spectrosc 40:183–190. doi:10.1002/jrs.2103

Shankar SS, Rai A, Ahmad A, Sastry M (2005) Controlling the optical properties of lemongrass extract synthesized gold nanotriangles and potential application in infrared-absorbing optical coatings. Chem Mater 17:566–572. doi:10.1021/cm048292g

Shaw CP, Fan M, Lane C, Barry G, Jirasek AI, Brolo AG (2013) Statistical correlation between SERS intensity and nanoparticle cluster size. J Phys Chem C 117:16596–16605. doi:10.1021/jp404250q

Shen JH, Yang XL, Zhu YH, Kang HG, Cao HM, Li CZ (2012) Gold-coated silica-fiber hybrid materials for application in a novel hydrogen peroxide biosensor. Biosens Bioelectron 34:132–136. doi:10.1016/j.bios.2012.01.031

Shen JH, Zhu YH, Yang XL, Zong J, Li CZ (2013) Multifunctional Fe_3O_4@Ag/SiO_2/Au core–shell microspheres as a novel SERS-activity label via long-range plasmon coupling. Langmuir 29:690–695. doi:10.1021/la304048v

Sosa IO, Noguez C, Barrera RG (2003) Optical properties of metal nanoparticles with arbitrary shapes. J Phys Chem B 107:6269–6275. doi:10.1021/jp0274076

Sun B, Han P, Zhao WX, Liu YH, Chen P (2014a) White-light-controlled magnetic and ferroelectric properties in multiferroic $BiFeO_3$ square nanosheets. J Phys Chem C 118:18814–18819. doi:10.1021/jp5064885

Sun B, Zhao WX, Wei LJ, Li HW, Chen P (2014b) Enhanced resistive switching effect upon illumination in self-assembled $NiWO_4$ nano-nests. Chem Commun 50:13142–13145. doi:10.1039/C4CC05784H

Wu DJ, Jiang SM, Liu XJ (2011) Tunable Fano resonances in three-layered bimetallic Au and Ag nanoshell. J Phys Chem C 115:23797–23801. doi:10.1021/jp209446p

Xu HX (2005) Multilayered metal core-shell nanostructures for inducing a large and tunable local optical field. Phys Rev B 72:073405. doi:10.1103/PhysRevB.72.073405

Zeng H, Sun SH (2008) Syntheses, properties, and potential applications of multicomponent magnetic nanoparticles. Adv Funct Mater 18:391–400. doi:10.1002/adfm.200701211

Zhang P, Guo YY (2009) Surface-enhancement Raman scattering inside metal nanoshells. J Am Chem Soc 131:3808–3809. doi:10.1021/ja8086642

Zhu J, Li JJ, Yuan L, Zhao JW (2012) Optimization of three-layered Au–Ag bimetallic nanoshells for triple-bands surface plasmon resonance. J Phys Chem C 116:11734–11740. doi:10.1021/jp301470p